# SAND Constraints for Theia

R. Petti

*University of South Carolina, Columbia SC, USA*

*Theia LBL meeting*
*17 March 2023*

# A TALE OF SYSTEMATICS

$$N_{\mathrm{X}}(E_{\mathrm{rec}}) = \int_{E_\nu} dE_\nu \, \Phi(E_\nu) \, P_{\mathrm{osc}}(E_\nu) \, \sigma_{\mathrm{X}}(E_\nu) \, R_{\mathrm{phys}}(E_\nu, E_{\mathrm{vis}}) \, R_{\mathrm{det}}(E_{\mathrm{vis}}, E_{\mathrm{rec}})$$

*Measurements expected to be dominated by systematics given intense LBNF beams.*

- *Dedicated measurements to constrain each factor with data*
- *Sensitivity of DUNE LBL analysis largely defined by control of systematics achievable*
  $\Longrightarrow$ *ND measurements critical to reduce LBL systematic uncertainties*
- *Required to demonstrate that ND can support precision LBL physics with Theia FD4*
  $\Longrightarrow$ *Need comparable or better LBL sensitivity as equivalent LAr FD*
- *Focus on Phase I ND complex: ND-LAr+TMS+SAND+PRISM optimized for LAr FD*
  $\Longrightarrow$ *Can the existing SAND detector be used as Theia ND?*

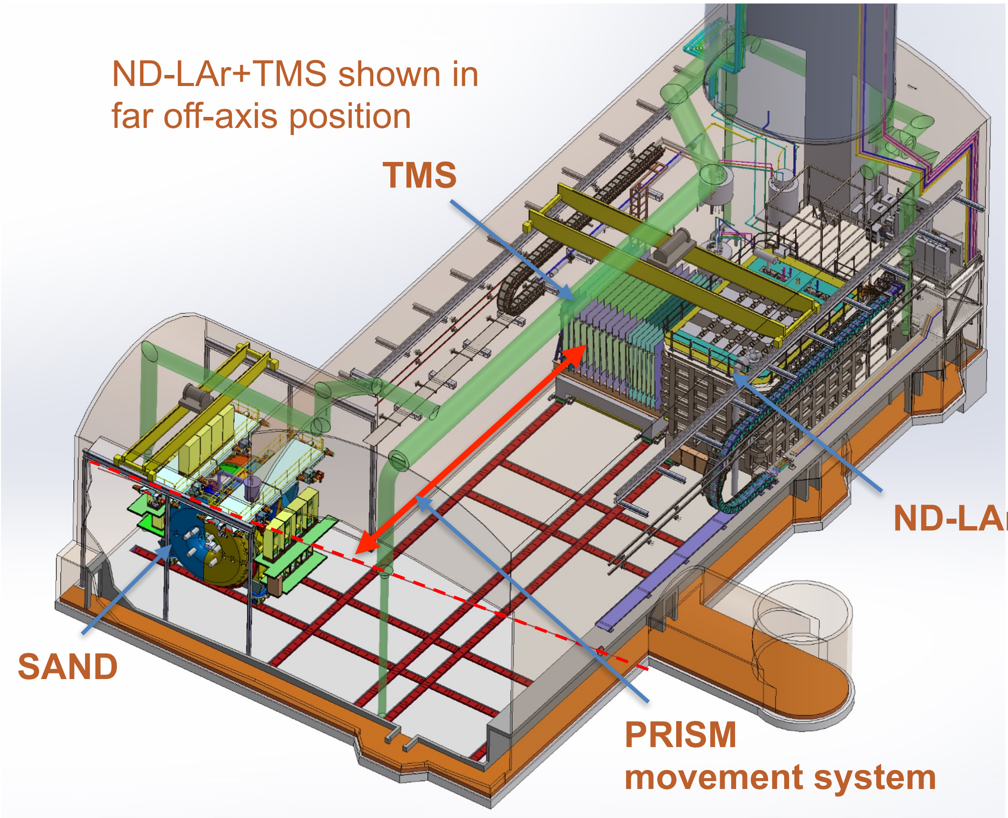


STT FV mass:
4.7 t $CH_2$
557 kg C

GRAIN mass:
1 t LAr

Front ECAL mass:
22.8 t Pb

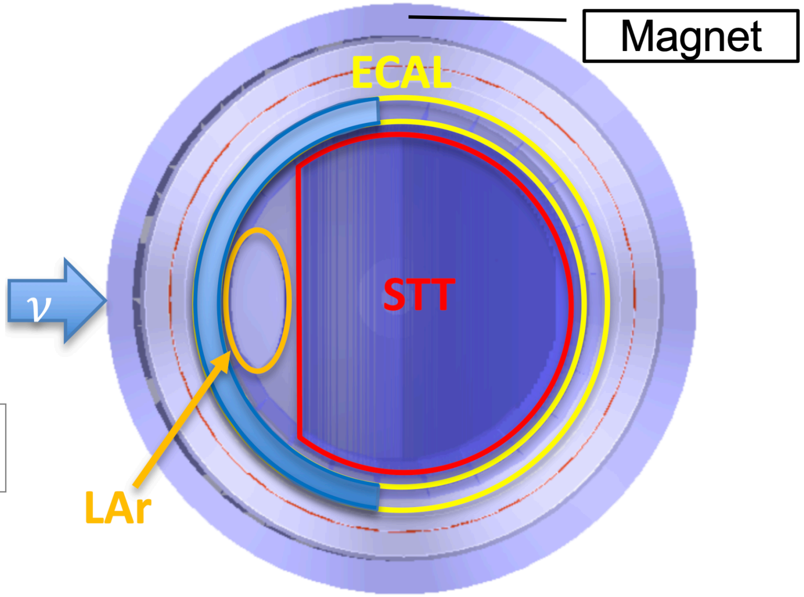


*Phase I ND: System for on-Axis Neutrino Detection (SAND) permanently on-axis*

# SYSTEMATICS FROM FLUX

$$N_X(E_{rec}) = \int_{E_\nu} dE_\nu \boxed{\Phi(E_\nu)} P_{osc}(E_\nu)\, \sigma_X(E_\nu)\, R_{phys}(E_\nu, E_{vis})\, R_{det}(E_{vis}, E_{rec})$$

$\boxed{\Delta\Phi(E_\nu)}$ *Flux uncertainties affect virtually every measurement in both ND and FD:*

- *Long-baseline oscillation analysis sensitive to spectral changes of on-axis flux;*
- *Flux and related uncertainties folded into all ND observables.*

$\Longrightarrow$ *Only factor which can be easily factored out in ND*

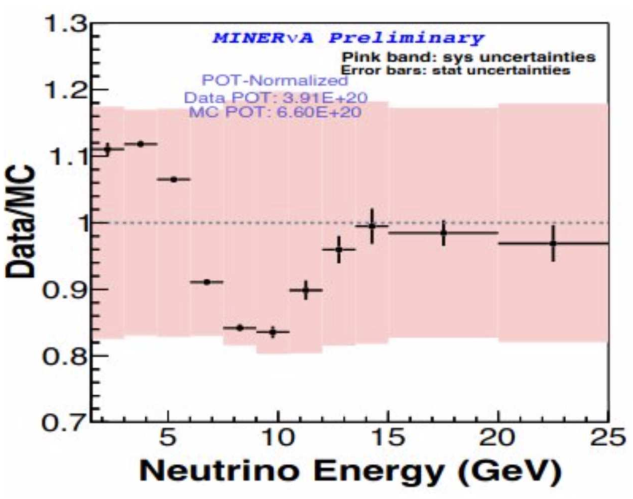


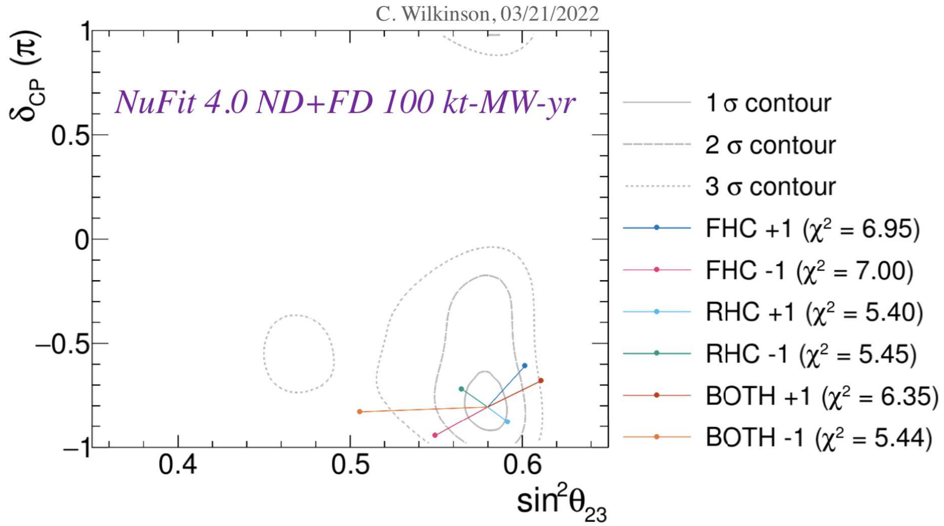

# FLUX MEASUREMENTS



$$N_X(E_{rec}) = \int_{E_\nu} dE_\nu \; \boxed{\Phi(E_\nu)} \; P_{osc}(E_\nu) \; \sigma_X(E_\nu) \; R_{phys}(E_\nu, E_{vis}) \; R_{det}(E_{vis}, E_{rec})$$

**H, $e^-$**

✦ *Measurements from ANY nuclear target limited by systematics from nuclear effects*

✦ *Relative flux vs. energy relevant for LBL analysis:*

- *SAND: relative $\nu_\mu$ and $\bar{\nu}_\mu$ flux from $\nu_\mu p \to \mu^- p \pi^+$ and $\bar{\nu}_\mu p \to \mu^+ n$ on H;*
- *ND-LAr & SAND: relative $\nu_\mu$ flux (limited info) from $\nu e^- \to \nu e^-$;*
- *SAND: $\nu_e/\nu_\mu$, $\bar{\nu}_e/\bar{\nu}_\mu$, and $\bar{\nu}_\mu/\nu_\mu$ ratios vs. energy.*

✦ *Absolute flux largely cancels out in LBL analysis based on $\nu_\mu, \bar{\nu}_\mu, \nu_e, \bar{\nu}_e$ CC samples:*

- *ND-LAr & SAND: absolute $\nu_\mu$ flux from $\nu e^- \to \nu e^-$;*
- *SAND: absolute $\bar{\nu}_\mu$ flux from $\bar{\nu}_\mu p \to \mu^+ n$ on H.*

# FLUX MEASUREMENTS WITH H

- *Relative $\nu_\mu$ flux vs. $E_\nu$ from exclusive $\nu_\mu p \to \mu^- p \pi^+$ on H:*
  $\nu < 0.5$ GeV *flattens cross-sections reducing uncertainties on $E_\nu$ dependence.*
- *Relative $\bar{\nu}_\mu$ flux vs. $E_\nu$ from exclusive $\bar{\nu}_\mu p \to \mu^+ n$ QE on H:*
  $\nu < 0.25$ GeV*: uncertainties comparable to relative $\nu_\mu$ flux from $\nu_\mu p \to \mu^- p \pi^+$ on H.*
- *Absolute $\bar{\nu}_\mu$ flux from QE $\bar{\nu}_\mu p \to \mu^+ n$ on H* with $Q^2 < 0.05$ GeV$^2$

$\Longrightarrow$ *Substantial reduction of systematics vs. techniques using nuclear targets*

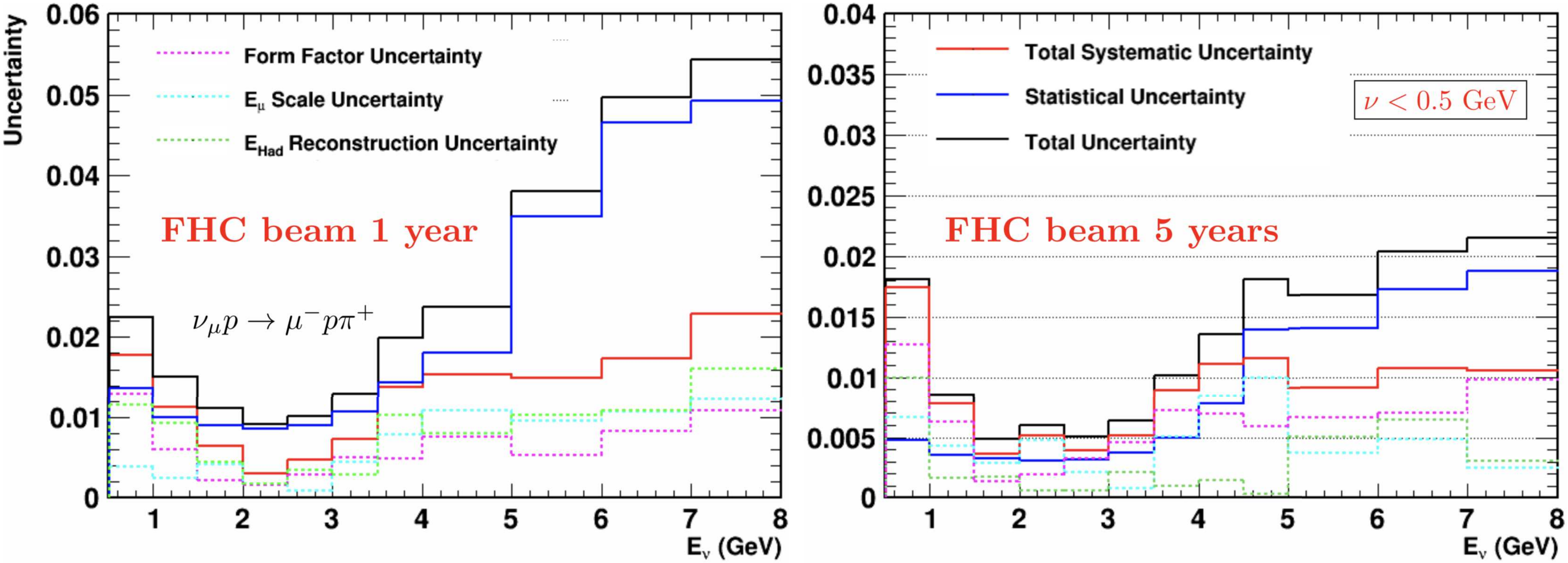

# SYSTEMATICS FROM NUCLEAR EFFECTS



$$N_X(E_{rec}) = \int_{E_\nu} dE_\nu \, \Phi(E_\nu) \, P_{osc}(E_\nu) \, \boxed{\sigma_X(E_\nu) \, R_{phys}(E_\nu, E_{vis})} \, R_{det}(E_{vis}, E_{rec})$$

$\sigma_X$ *Cross-section on C and O targets (nuclear effects) required for Theia*

$R_{phys}$ *Smearing introduced by nuclear effects on initial and final state particles results in systematics on* $\boxed{\Delta E_\nu \text{ SCALE}}$ *since* $E_\nu$ *unknown on event-by-event basis.*

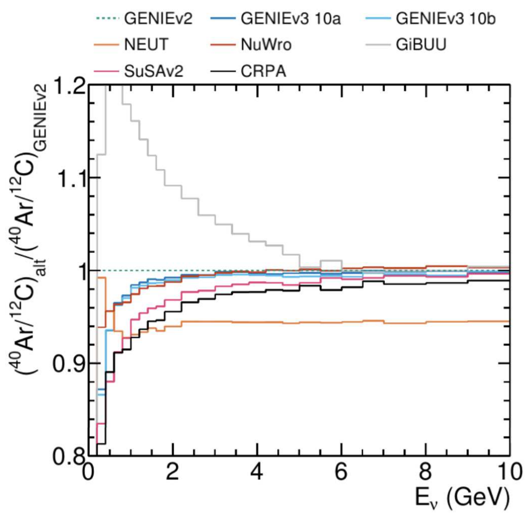


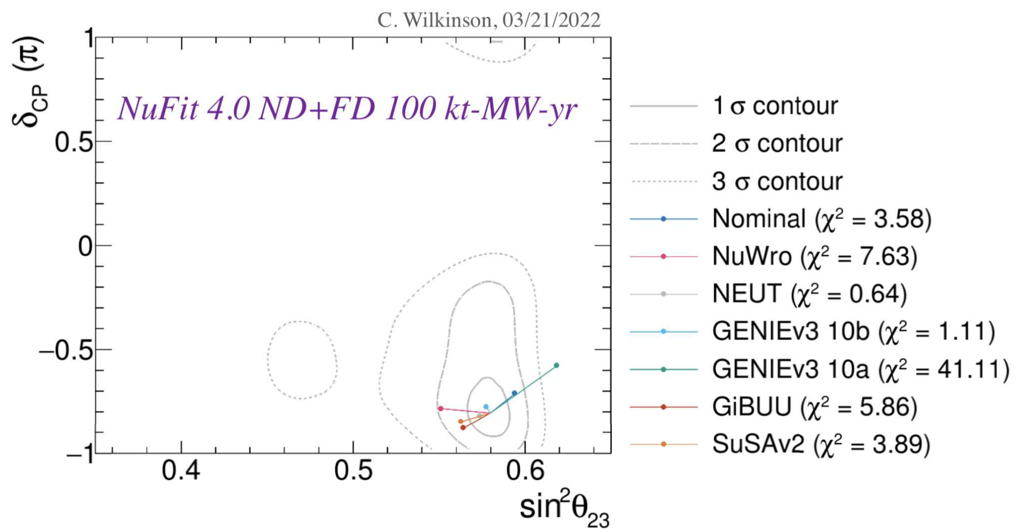

# CROSS-SECTION MEASUREMENTS ON C,O,$H_2O$

$$N_X(E_{rec}) = \int_{E_\nu} dE_\nu \; \Phi(E_\nu) \; P_{osc}(E_\nu) \; \boxed{\sigma_X(E_\nu) \; R_{phys}(E_\nu, E_{vis})} \; R_{det}(E_{vis}, E_{rec})$$

**SAND**

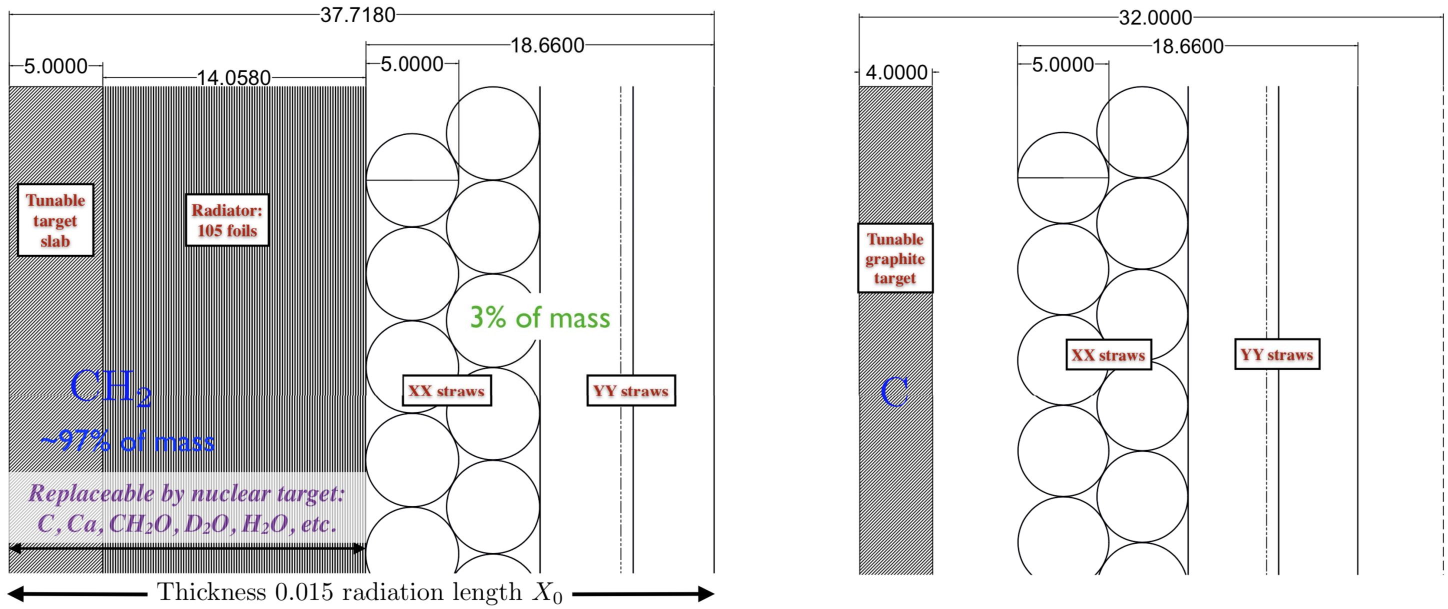


- *Many (70-80) thin (1-2% $X_0$) passive targets* separated from active detector (straw layers);
- *Targets of high chemical purity ($\sim 97\%$ of mass)* keeping average density $\rho \leq 0.18$ g/cm$^3$
- *High track sampling*: 0.15 (0.36)%$X_0$ $\perp$ ($\parallel$) with total detector thickness $\sim 1.3 X_0$;
- *"Solid" hydrogen target* from a subtraction of $CH_2$ & C targets.

# CROSS-SECTION MEASUREMENTS ON C,O,$H_2O$



$$N_{\rm X}(E_{\rm rec}) = \int_{E_\nu} dE_\nu \; \Phi(E_\nu) \; P_{\rm osc}(E_\nu) \; \boxed{\sigma_{\rm X}(E_\nu) \; R_{\rm phys}(E_\nu, E_{\rm vis})} \; R_{\rm det}(E_{\rm vis}, E_{\rm rec})$$

↓

**SAND**

✦ *Cross-sections & related nuclear smearing on integrated pure C (graphite) target*

✦ *Cross-sections & related nuclear smearing on "solid" oxygen target:*

$$N_{\rm O}(\vec{x}) \equiv N_{\rm CH_2O}(\vec{x}) - \frac{M_{\rm CH_2/CH_2O}}{M_{\rm CH_2}} N_{\rm CH_2}(\vec{x})$$

- *Exploit unique STT feature: thin passive targets can be replaced during data taking;*
- *Interactions on oxygen from subtraction between polyoxymethylene (delrin) and default $CH_2$ targets. Oxygen content by mass within delrin is dominant at 53.3%, excellent mechanical properties.*

✦ *Detailed characterization of inclusive & exclusive topologies on C and O:*

- *CC interactions from different flavor components of beam;*
- *Pion and hadron multiplicity measurements expected from MCND, etc.*
- *Background processes for LBL: NC interactions, $\pi^0$ and $\gamma$, meson decays, etc.*

| Target material | Composition | Density | Thickness | Rad. length | Nucl. int. length |
|---|---|---|---|---|---|
| Polypropylene | $CH_2$ | $0.91\ g/cm^3$ | 7.0 mm | $0.015\ X_0$ | $0.008\ \lambda_I$ |
| Graphite | C | $1.80\ g/cm^3$ | 4.0 mm | $0.016\ X_0$ | $0.008\ \lambda_I$ |
| Polyoxymethylene | $CH_2O$ | $1.41\ g/cm^3$ | 4.5 mm | $0.016\ X_0$ | $0.008\ \lambda_I$ |

✦ *Cross-sections on water target:*

$$N_{\rm H_2O}(\vec{x}) \equiv N_{\rm CH_2O}(\vec{x}) - \frac{M_{\rm C/CH_2O}}{M_{\rm C}} N_{\rm C}(\vec{x})$$

- *Exploit simultaneous presence of alternated $CH_2$, C, and $CH_2O$ targets in STT.*
- *Interactions on water from subtraction between polyoxymethylene ($CH_2O$) and graphite (C) targets. Water content by mass within delrin is 60%, mass of available C targets larger than C in delrin.*

✦ *Thin passive water targets can also be integrated in STT:*

- *Water layers 12 mm thick encapsulated within 1.5 mm delrin shells, corresponding to 0.044 $X_0$;*
- *Background from C to be subtracted with graphite targets only 10.4%.*

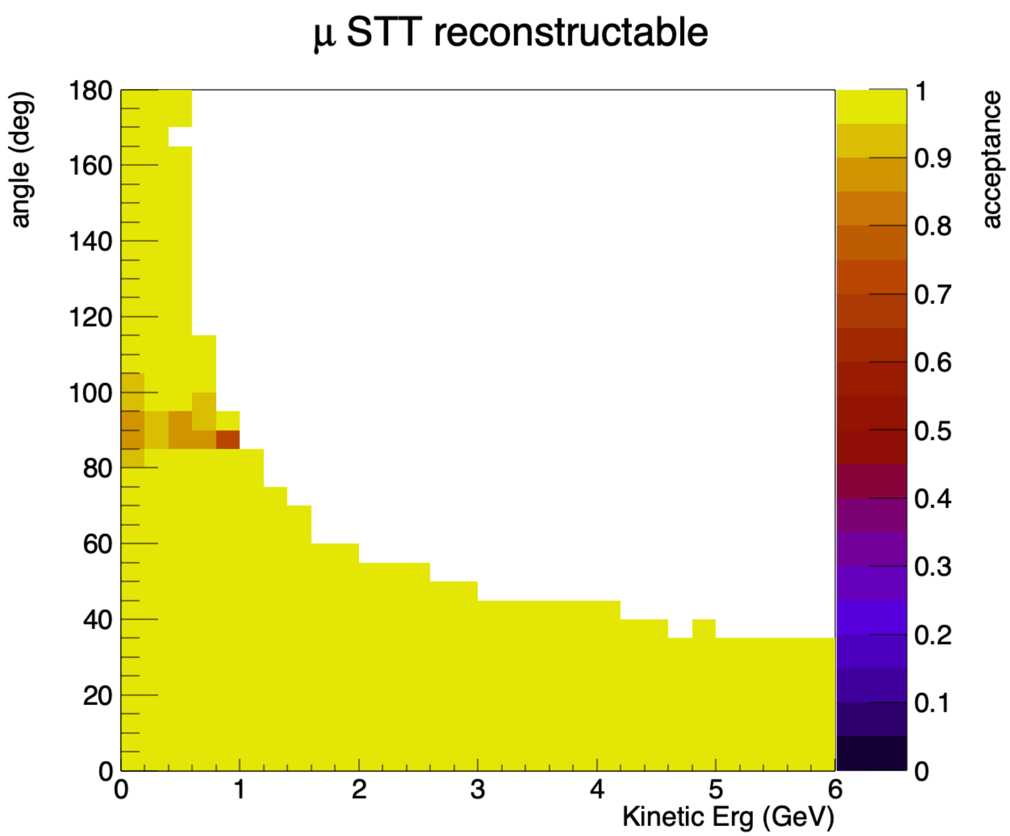


*Integrated over all angles*

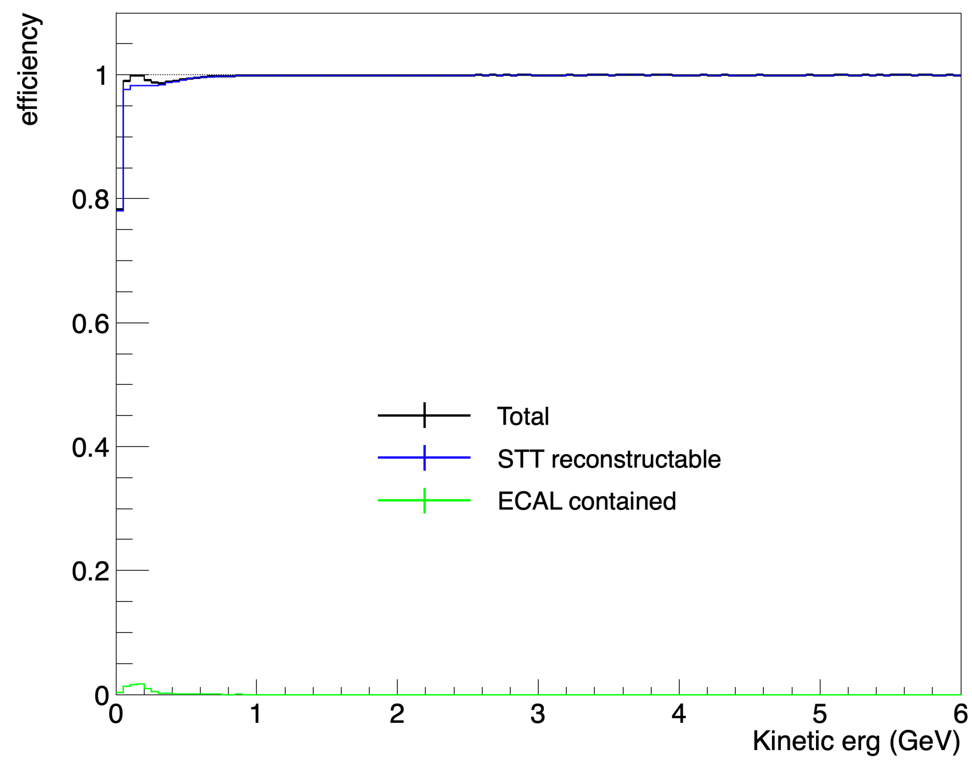


*SAND can provide high statistics samples of interactions on H, C, O (& $H_2O$)*
*with large acceptance over the full 4π angle down to low momenta ($\rho < 0.18$ g/cm$^3$)*

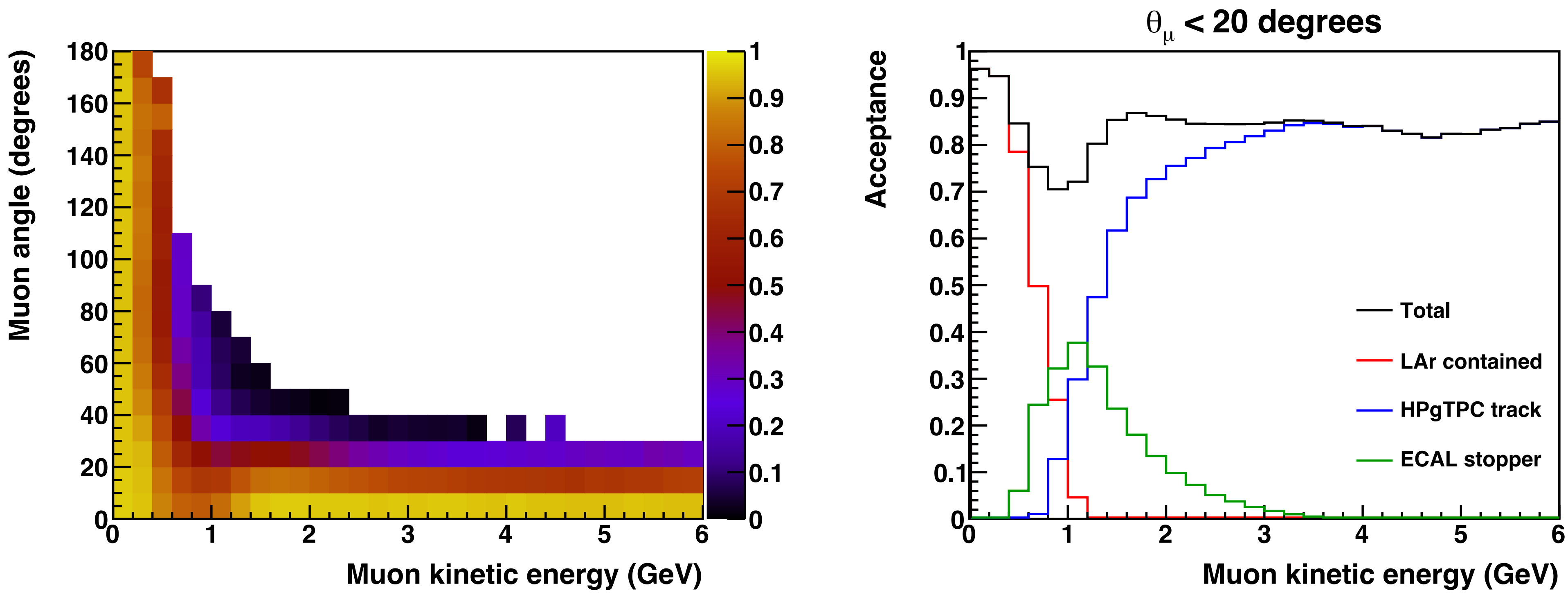


*Muon acceptance for ND-LAr+ND-GAr (Phase II) from ND CDR*

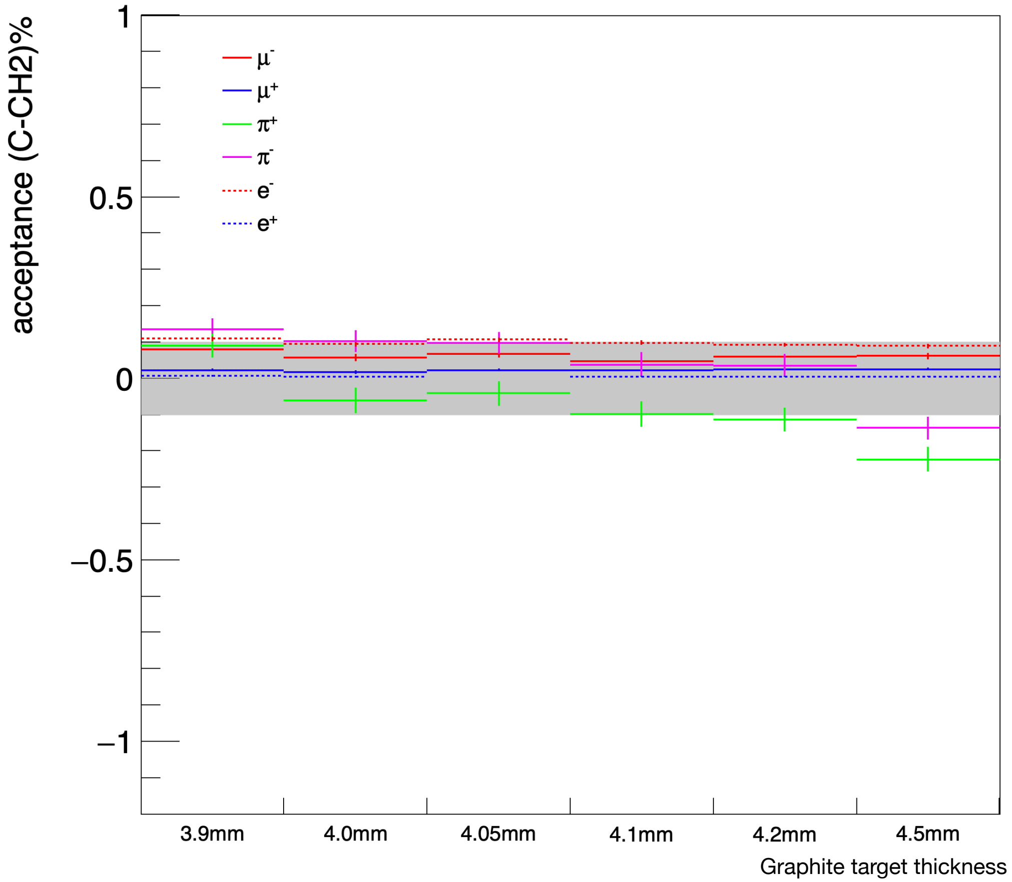


*Optimization of the ratio between the $CH_2$ and C thickness shows that we can keep acceptance differences among $CH_2$, C, $CH_2O$ targets $<10^{-3}$ for all particles*

# CALIBRATION OF $E_\nu$ SCALE WITH H

$$N_X(E_{rec}) = \int_{E_\nu} dE_\nu \, \boxed{\Phi(E_\nu)} \, P_{osc}(E_\nu) \, \boxed{\sigma_X(E_\nu)} \, \boxed{R_{phys}(E_\nu, E_{vis})} \, \boxed{R_{det}(E_{vis}, E_{rec})}$$

$\Phi(E_\nu)$ → **$\sim$1% in H**; $\sigma_X(E_\nu)$ → $F_i(Q^2)$; $R_{phys}(E_\nu, E_{vis})$ → $R_{phys} \equiv I$; $R_{det}(E_{vis}, E_{rec})$ → $K_0, \Lambda, \gamma$

- *Combination of $\nu$-H & $\bar{\nu}$-H CC calibration sample for (anti)neutrino energy scale* $\boxed{\Delta E_\nu}$
- *Compare with CC inclusive interactions on C and O targets*
  $\Longrightarrow$ *Same detector acceptance in STT*
- *Calibration using $y$ distribution (minimal nuclear effects on $\sigma$)*
- *Understanding nuclear smearing required to reduce unfolding systematics*

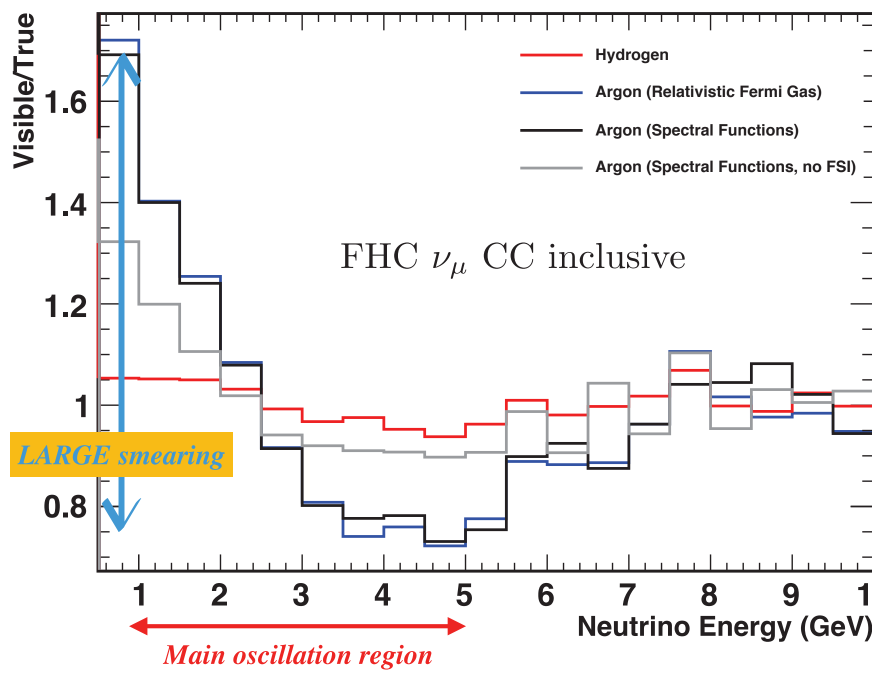

# MULTIPLICITIES & EVENT TOPOLOGY

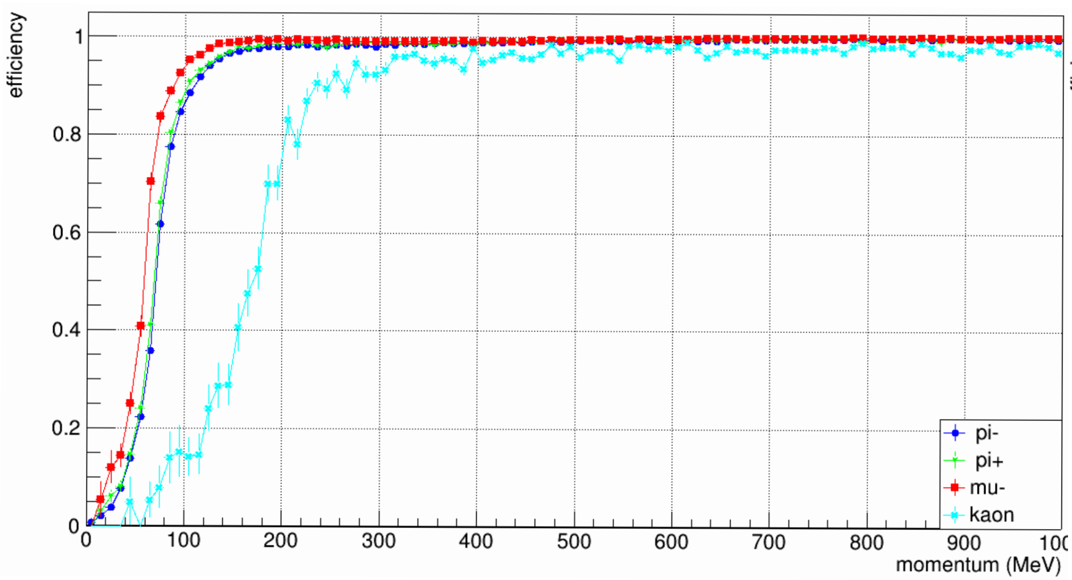


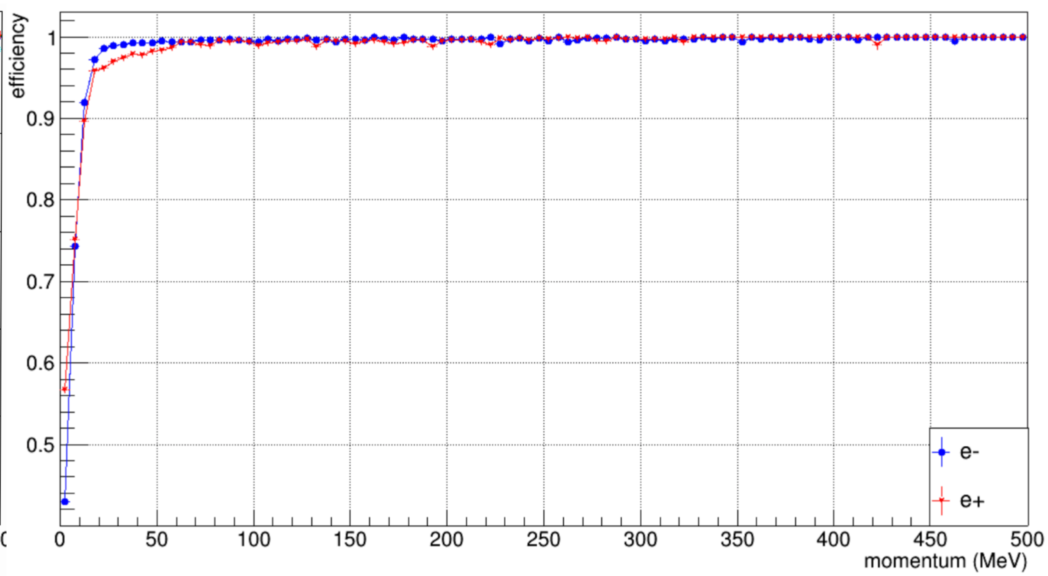


*Low-density design and excellent particle ID capabilities allows SAND to measure visible final state particles down to low momenta*

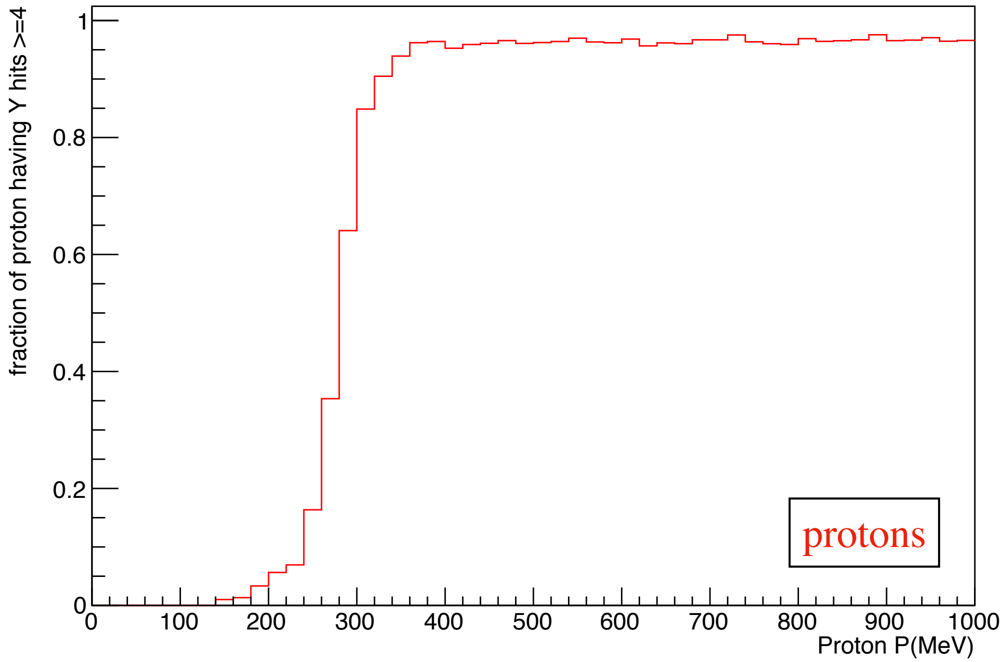


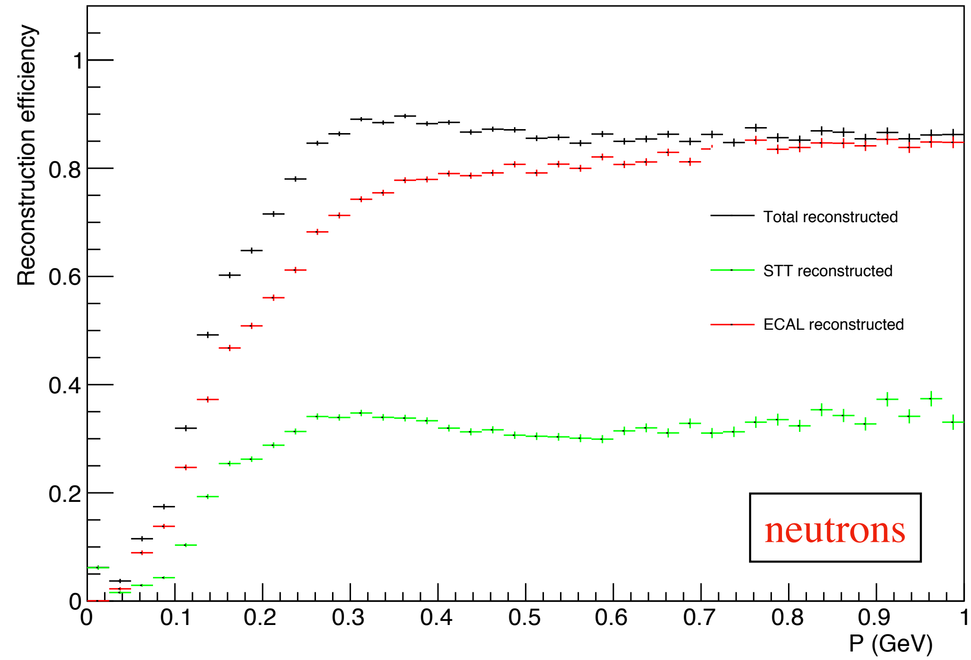


*Low-density design and excellent particle ID capabilities allows SAND to measure visible final state particles down to low momenta*

DUNE Snowmass white paper

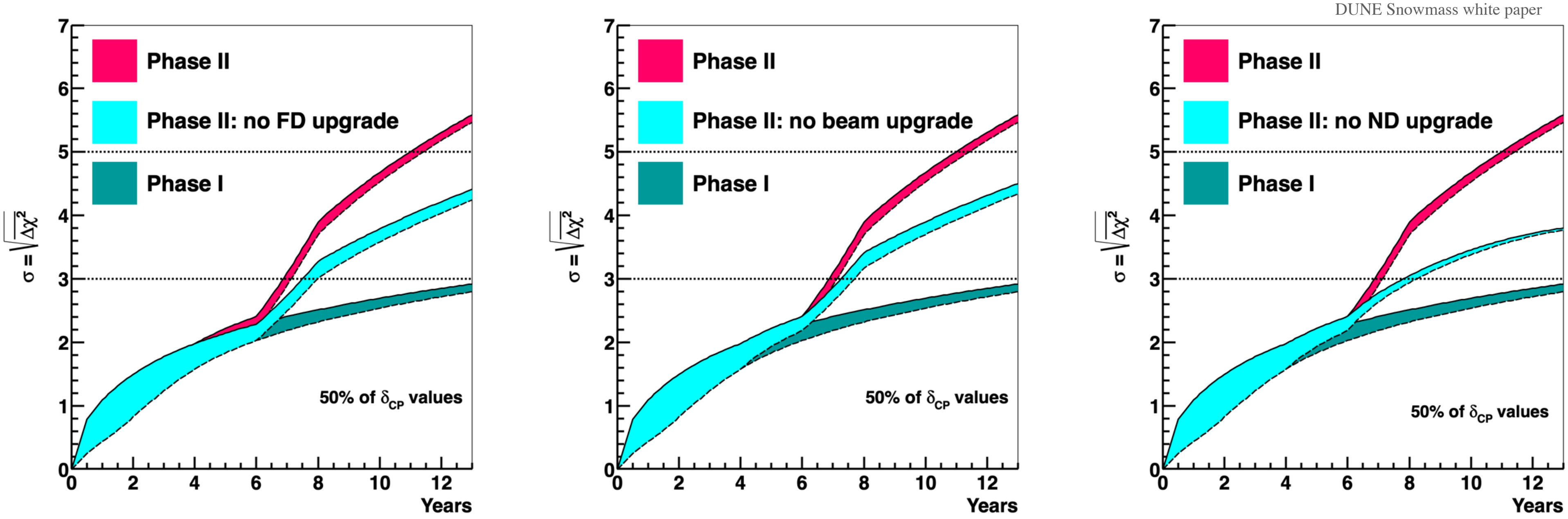


*Addition of ND-GAr in Phase II provides detailed measurements of hadron multiplicities on Ar extending the DUNE LBL sensitivity for LAr*

$\Longrightarrow$ *SAND can provide similar measurements on C,O,$H_2O$ for Theia*

# ACHIEVABLE STATISTICS



- *With default 1.2 MW beam a 1 tonne $H_2O$ target will collect:*
  *$1.4\times10^6$ $\nu_\mu$ CC/year (FHC) and $0.5\times10^6$ $\bar{\nu}_\mu$ CC/year (RHC)*

- *Replacing 20 $CH_2$ targets (out of 70 total) with solid delrin slabs in STT would provide an oxygen target of $\sim$600 kg, comparable with the available mass of C and H*

  $\Longrightarrow$ *Straightforward and relatively inexpensive to implement*

- *A water target close to 1 tonne can be easily achieved with a combination of delrin slabs (20 slabs equivalent to about 700 kg $H_2O$) and thin water targets (for cross-check)*

  $\Longrightarrow$ *Statistics adequate to expected systematics from energy scale & flux*

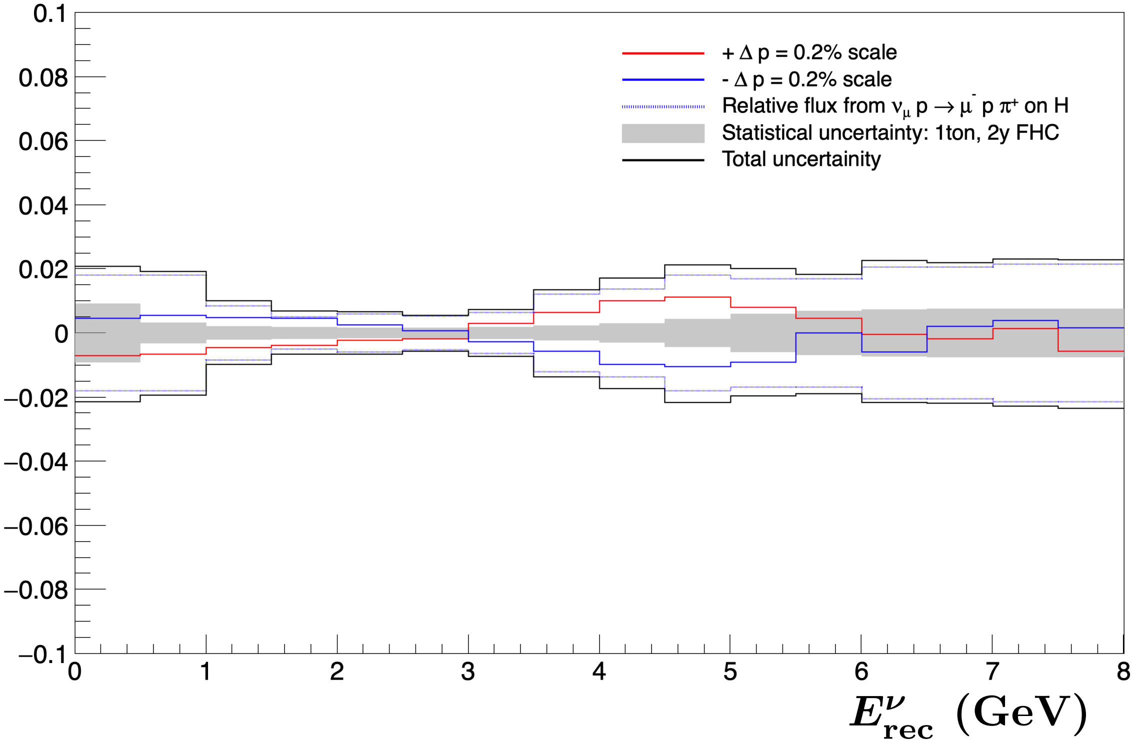


*With a 2y FHC 1.2 MW exposure uncertainties dominated by systematics even for a relatively small 1 ton target in SAND*

# CALIBRATION OF DETECTOR RESPONSE



$$N_{\rm X}(E_{\rm rec}) = \int_{E_\nu} dE_\nu \; \Phi(E_\nu) \; P_{\rm osc}(E_\nu) \; \sigma_{\rm X}(E_\nu) \; R_{\rm phys}(E_\nu, E_{\rm vis}) \; \boxed{R_{\rm det}(E_{\rm vis}, E_{\rm rec})}$$

$R_{\rm det}$ *Detector smearing controlled by* $\boxed{\Delta E \text{ SCALE}}$ *and reconstruction efficiencies.*

✦ *Requires "identical" technology as in FD: differences in rates, event containment,* $E_\nu$ *energy spectra, etc. between ND and FD imply sizable (model) corrections*

- *SAND can accurately measure fraction of tracks/energy above Cherenkov threshold;*
- *SAND measures final state particles down to low thresholds guiding scintillation light estimate.*

$\Longrightarrow$ *Does Theia need large WbLS detector with optical readout within ND?*

✦ *For the calibration of the FD response various constraints can be considered:*

- *Dedicated testbeam exposure of smaller WbLS optical detector;*
- *In-situ FD calibration: laser Wakefield acceleration (M. Mooney),*
  *FD control samples from athmospheric neutrinos, cosmics, or beam-related events;*
- *Experience from existing detectors based on a similar technology (e.g. Super-K).*

# SUMMARY



- ✦ *DUNE Phase I ND complex is optimized for LAr FD but SAND can provide valuable ND constraints for a Theia FD4 in Phase II*
  $\Longrightarrow$ *Use of existing ND component can mitigate risks for the Theia LBL program*

- ✦ *In-situ flux measurements are target-independent and are expected to be dominated by precision measurements using exclusive processes on H in SAND, with additional contributions from $\nu$-e scattering in both ND-LAr and SAND.*

- ✦ *Detailed characterization of event topologies on C and O (& $H_2O$) possible in SAND:*
  - *Cross-section measurements for inclusive and exclusive processes on C and O;*
  - *Nuclear effects & related smearing for C and O targets;*
  - *Calibration of $E_\nu$ scale from comparison with interactions on H with similar detector acceptance.*

- ✦ *Need to evaluate FD reconstruction systematics and possible calibration strategies*
  $\Longrightarrow$ *Does the Theia LBL program require an additional "identical" ND component?*

# Backup slides

# EXPECTED STATISTICS IN SAND

| Target | CP optimized FHC (1.2MW, 2y) | | | | CP optimized RHC (1.2MW, 2y) | | | |
|---|---|---|---|---|---|---|---|---|
| | $\nu_\mu$ CC | $\bar{\nu}_\mu$ CC | $\nu_e$ CC | $\bar{\nu}_e$ CC | $\nu_\mu$ CC | $\bar{\nu}_\mu$ CC | $\nu_e$ CC | $\bar{\nu}_e$ CC |
| $CH_2$ | 13,010,337 | 624,330 | 192,118 | 31,902 | 2,035,973 | 4,870,562 | 91,004 | 69,278 |
| H | 1,222,576 | 111,574 | 18,396 | 5,557 | 194,216 | 906,130 | 8,712 | 12,434 |
| C | 1,547,011 | 67,294 | 22,799 | 3,458 | 241,710 | 520,287 | 10,800 | 7,460 |
| Ar | 3,114,331 | 121,506 | 46,384 | 6,503 | 480,862 | 936,489 | 21,932 | 13,867 |
| Pb | 62,127,600 | 2,507,940 | 923,012 | 130,680 | 10,375,400 | 18,222,200 | 437,284 | 265,304 |

*NOTE: 100 kt-MW-years in Phase I FD corresponds to about 2y FHC + 2y RHC with 1.2 MW beam*

STT FV mass:
4.7 t $CH_2$
557 kg C

GRAIN mass:
1 t LAr

Front ECAL mass:
22.8 t Pb

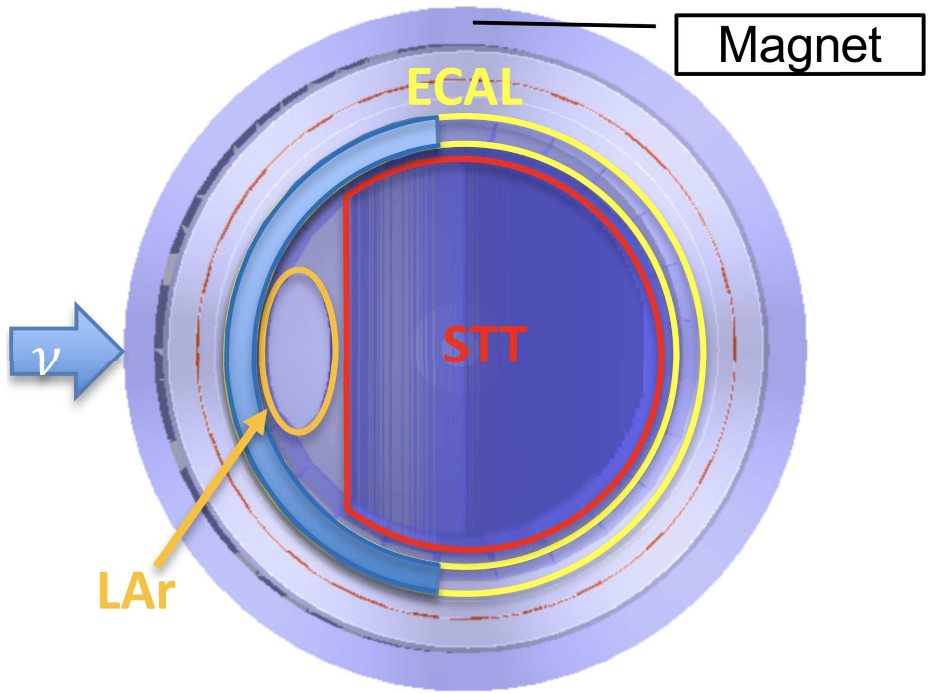

# A TOOL TO REDUCE SYSTEMATICS

- *STT designed to offer a control of $\nu$-target(s) similar to $e^{\pm}$ DIS experiments:*
  - *Thin (1-2% $X_0$) passive target(s) separated from active detector (straw layers);*
  - *Target layers spread out throughout tracker by keeping low density* $0.005 \leq \rho \leq 0.18$ *g/cm$^3$*.
  - *Replaceable targets of high chemical purity give $\sim 97\%$ of STT mass (straws 3%).*

$\Longrightarrow$ *STT target configuration can be fully tuned/configured*

- *Low-density design & target mass allow accurate in-situ calibrations:*
  - $\Delta p < 0.2\%$ *momentum scale uncertainty from $K_0 \to \pi^+\pi^-$ in STT volume (337,000 in FHC);*
  - *p reconstruction and identification, vertex, etc. from $\Lambda \to p\pi^-$ in STT volume (506,000 in FHC);*
  - *$e^{\pm}$ reconstruction and identification from $\gamma \to e^+e^-$ in STT volume ($8 \times 10^6$ in FHC).*

- *SAND multipurpose detector with combined particle ID & tracking:*
  - *Electron ID with Transition Radiation and dE/dx in STT + ECAL energy and topology;*
  - *$4\pi$ detection of $\pi^0$ from $\gamma$ conversions ($\sim 49\%$) within the STT volume + ECAL clusters;*
  - *$p/\pi/K$ ID with dE/dx, range, time-of-flight with ECAL, and ECAL energy depositions.*

- *Accurate reconstruction of transverse plane kinematics from particle 4-momenta:*
  - *"Transparent" target/tracker system with total length* $\sim 1.3 X_0$;
  - *NOMAD concept originally developed for kinematic detection of $\nu_\tau$ [Nucl.Phys.B 611 (2001) 3-39].*

*Hyper-Kamiokande Design Report, arXiv:1805.04163 [physics.ins-det]*

| | | Flux & ND-constrained cross section | ND-independent cross section | Far detector | Total |
|---|---|---|---|---|---|
| $\nu$ mode | Appearance | 3.0% | 0.5% | 0.7% | 3.2% |
| | Disappearance | 3.3% | 0.9% | 1.0% | 3.6% |
| $\overline{\nu}$ mode | Appearance | 3.2% | 1.5% | 1.5% | 3.9% |
| | Disappearance | 3.3% | 0.9% | 1.1% | 3.6% |

*Uncertainties on expected events from FD efficiency and reconstruction sub-leading in Hyper-Kamiokade*

# “SOLID” HYDROGEN TARGET

✦ “Solid” Hydrogen concept: $\nu(\bar{\nu})$-H from subtraction of $CH_2$ & C targets

- Exploits high resolutions & control of chemical composition and mass of targets in STT;
- Model-independent data subtraction of dedicated C (graphite) target from main $CH_2$ target;

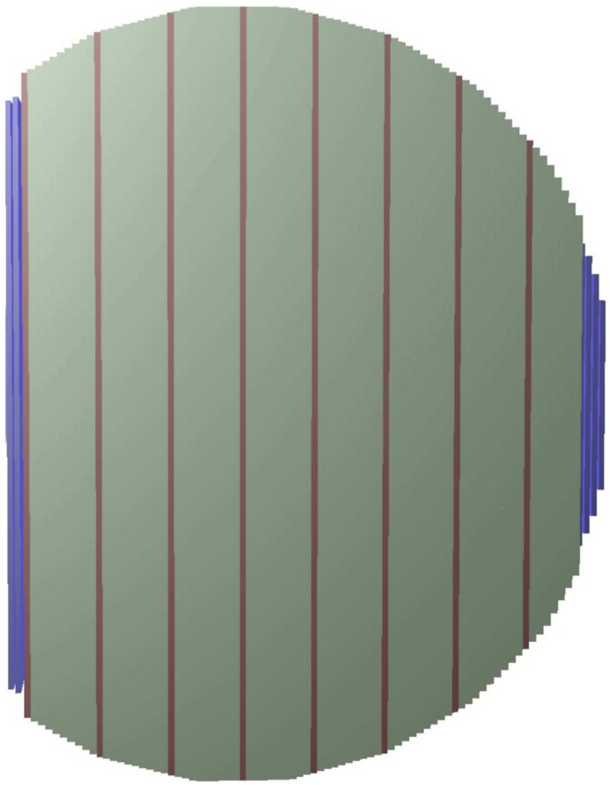

Green: $CH_2$ Brown: C

Similar thickness 1-2% $X_0$
for both $CH_2$ and C

$CH_2$ and C targets alternated in FV
to guarantee same acceptance

Mass ratio optimized for subtraction

$\Longrightarrow$ Equivalent to about $10\ \mathrm{m}^3\ \mathrm{LH}_2$

# "SOLID" HYDROGEN TARGET

✦ *"Solid" Hydrogen concept: $\nu(\bar{\nu})$-H from subtraction of* CH$_2$ & C *targets*

- *Exploits high resolutions & control of chemical composition and mass of targets in STT;*
- *Model-independent data subtraction of dedicated C (graphite) target from main CH$_2$ target;*
- *Kinematic selection can reduce dilution factor for inclusive & exclusive CC topologies with 80-95% purity and 75-96% efficiency before subtraction.*

$\Longrightarrow$ *Viable and acceptable approximation to liquid H$_2$ detectors*

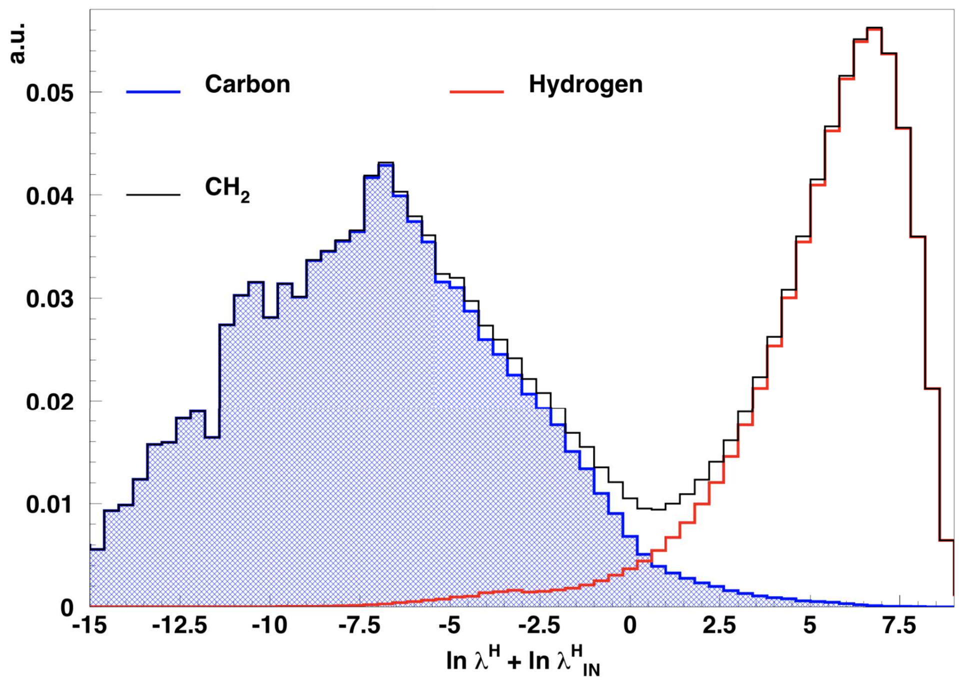


| CC process (1y+1y) | H selected Evts/year |
|---|---|
| $\nu_\mu p \to \mu^- p \pi^+$ | 408,000 |
| $\nu_\mu p \to \mu^- p \pi^+ X$ | 152,000 |
| $\nu_\mu p \to \mu^- n \pi^+ \pi^+ X$ | 19,000 |
| $\nu_\mu$ CC inclusive on H | 579,000 |
| $\bar{\nu}_\mu p \to \mu^+ n$ | 172,000 |
| $\bar{\nu}_\mu p \to \mu^+ p \pi^-$ | 61,000 |
| $\bar{\nu}_\mu p \to \mu^+ n \pi^0$ | 42,000 |
| $\bar{\nu}_\mu p \to \mu^+ p \pi^- X$ | 27,000 |
| $\bar{\nu}_\mu p \to \mu^+ n \pi \pi X$ | 31,000 |
| $\bar{\nu}_\mu$ CC inclusive on H | 333,000 |

# SUMMARY OF FLUX MEASUREMENTS

- *Relative $\nu_\mu$ flux vs. $E_\nu$ from exclusive $\nu_\mu p \to \mu^- p \pi^+$ on Hydrogen:* $< 1\%$
  $\nu < 0.5$ GeV *flattens cross-sections reducing uncertainties on $E_\nu$ dependence.*

- *Relative $\bar{\nu}_\mu$ flux vs. $E_\nu$ from exclusive $\bar{\nu}_\mu p \to \mu^+ n$ QE on Hydrogen:* $< 1\%$
  $\nu < 0.25$ GeV*: uncertainties comparable to relative $\nu_\mu$ flux from $\nu_\mu p \to \mu^- p \pi^+$ on H.*

- *Absolute $\nu_\mu$ flux from $\nu e^- \to \nu e^-$ elastic scattering:* $< 2\%$
  $\Longrightarrow$ *Complementary to measurement in LAr TPC with small systematics*

- *Absolute $\bar{\nu}_\mu$ flux from QE $\bar{\nu}_\mu p \to \mu^+ n$ on H with* $Q^2 < 0.05$ GeV$^2$*: $\sim$ 27k/year in RHC*

- *Ratio of $\nu_e/\nu_\mu$ AND $\bar{\nu}_e/\bar{\nu}_\mu$ vs. $E_\nu$ from $CH_2$ (& H) targets*
  $\Longrightarrow$ *Excellent $e^\pm$ charge measurement and $e^\pm$ identification ($\sim$ 16k/year $\bar{\nu}_e$ CC in FHC)*

- *Ratio of $\bar{\nu}_\mu/\nu_\mu$ vs. $E_\nu$ from coherent $\pi^-/\pi^+$ on C ($CH_2$ and C): 3.5-7%*
  $\Longrightarrow$ *Excellent angular resolution (t variable) and light isoscalar target*

- *Determination of parent $\mu/\pi/K$ distributions from $\nu(\bar{\nu})$-H (& $CH_2$) at low-$\nu$*
  $\Longrightarrow$ *Direct in-situ measurement for flux extrapolation to FD*

## *Impact of relative flux uncertainty on ND observables*

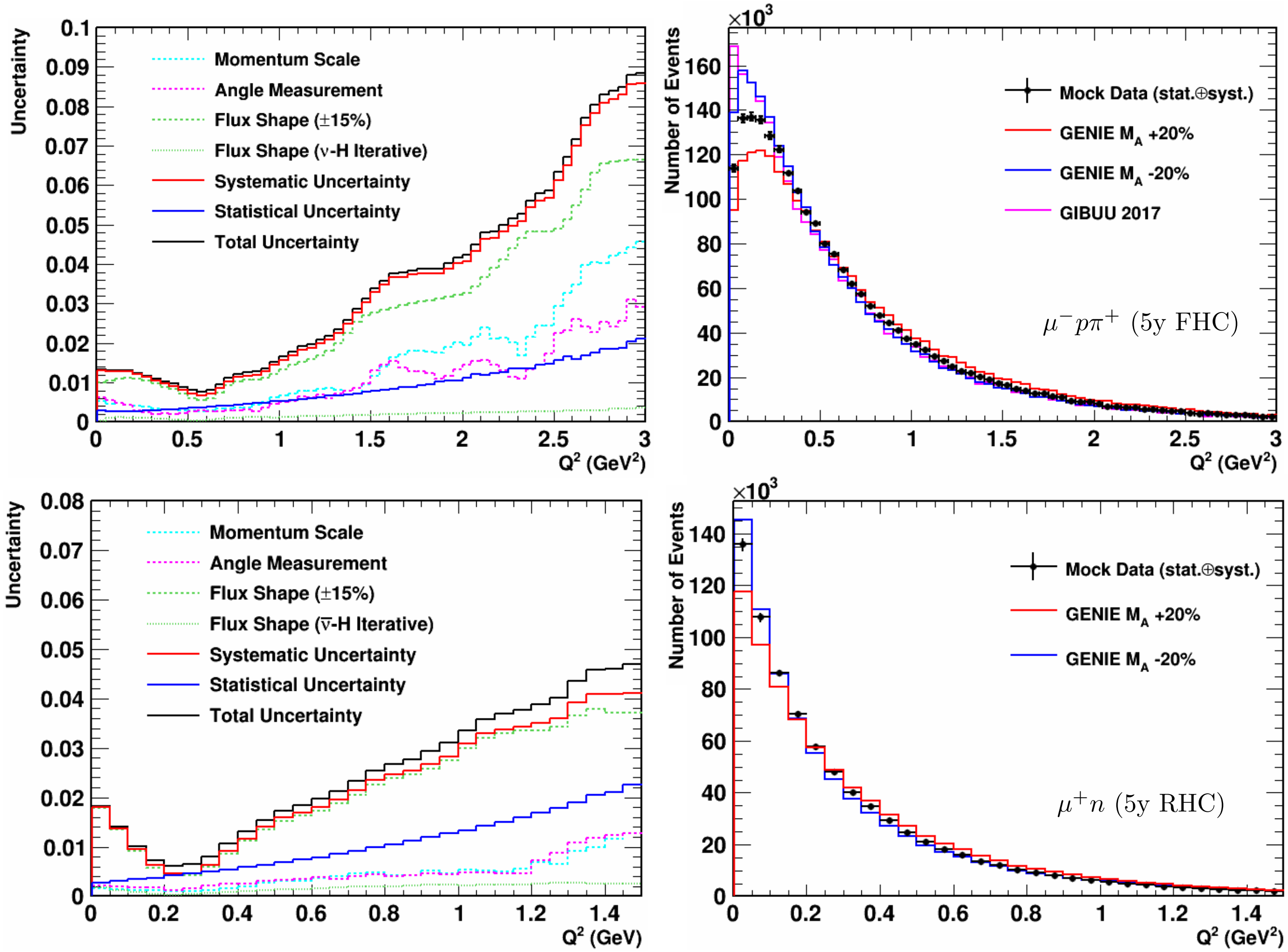


Expected $Q^2$ distributions for $\nu_\mu p \to \mu^- p \pi^+$ and $\bar{\nu}_\mu p \to \mu^+ n$ on H

*Impact of relative flux uncertainty on ND observables*

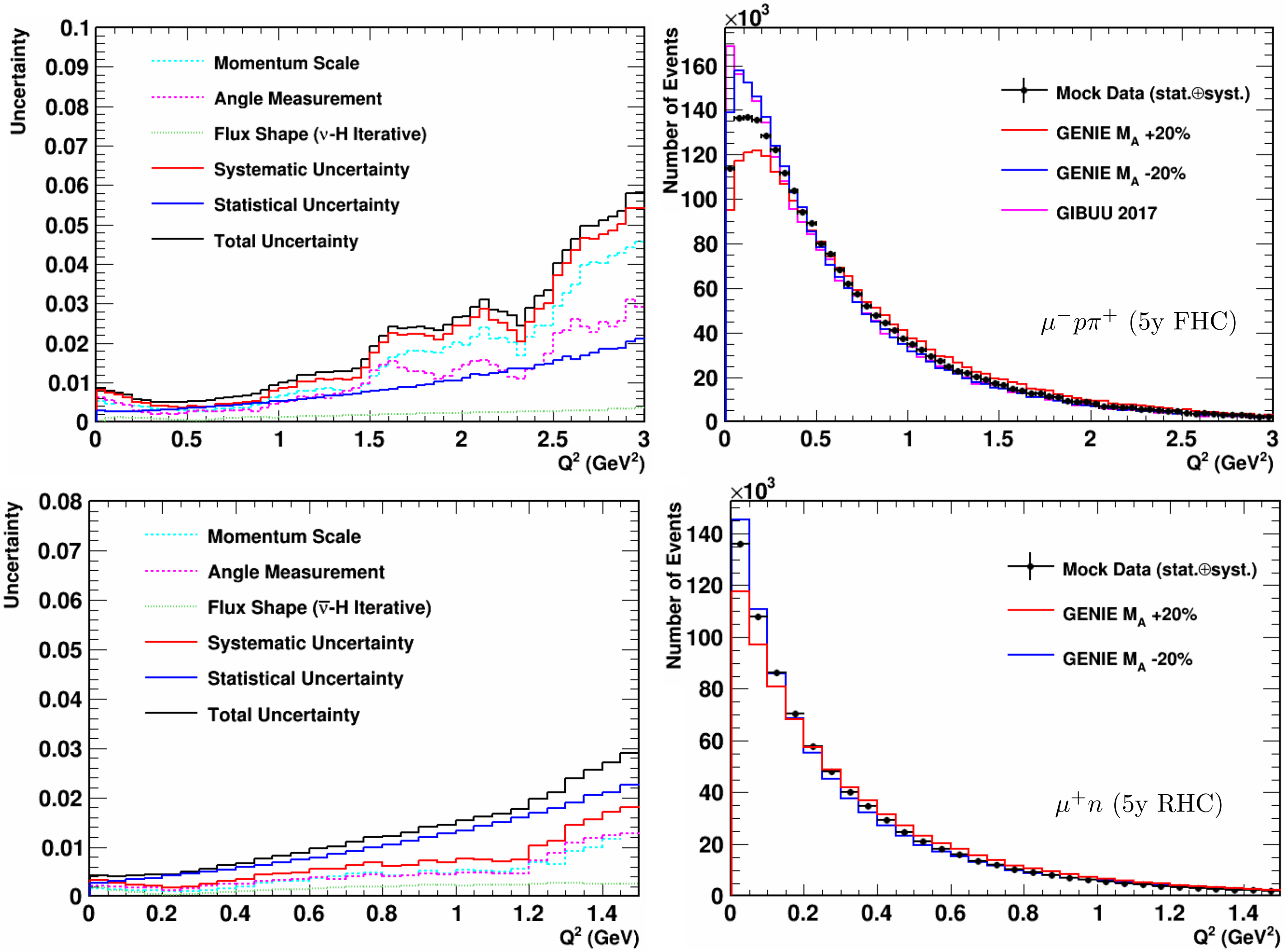


Expected $Q^2$ distributions for $\nu_\mu p \to \mu^- p \pi^+$ and $\bar{\nu}_\mu p \to \mu^+ n$ on H

# BEAM FLAVOR COMPOSITION

| Event type | Efficiency | Purity $(\nu_\mu+\bar{\nu}_\mu+\nu_e+\bar{\nu}_e)$ CC+NC | Wrong sign contamination |
|---|---|---|---|
| **Tagging + WS veto + $\mu^\pm$ ID:** | | | |
| FHC $\nu_\mu$ CC with tagged $\mu^-$ | 98.4 % | 97.5 % | 0.5 % |
| RHC $\bar{\nu}_\mu$ CC with tagged $\mu^+$ | 97.9 % | 97.8 % | 0.3 % |
| RHC $\nu_\mu$ CC with tagged $\mu^-$ | 95.4 % | 97.3 % | 0.3 % |
| FHC $\bar{\nu}_\mu$ CC with tagged $\mu^+$ | 95.4 % | 94.2 % | 2.6 % |
| **Tagging + muon veto + $e^\pm$ ID:** | | | |
| FHC $\nu_e$ CC with tagged $e^-$ | 82.6 % | 99.4 % | |
| RHC $\bar{\nu}_e$ CC with tagged $e^+$ | 83.8 % | 99.2 % | |
| RHC $\nu_e$ CC with tagged $e^-$ | 82.0 % | 99.3 % | |
| FHC $\bar{\nu}_e$ CC with tagged $e^+$ | 84.3 % | 93.6 % | |

- *CC selections based on kinematic tagging, wrong sign (WS) veto, and $\mu^\pm(e^\pm)$ ID:* for specific processes/topologies (e.g. CC on H) additional background rejection.

- *Large acceptance for CC leptons:* 99.7% (99.9%) to reconstruct $\mu^-$ FHC ($\mu^+$ RHC).
  $\Longrightarrow$ *Small MC corrections reduce model-dependent systematics*

# ABSOLUTE $\nu_\mu$ FLUX WITH $\nu e^- \to \nu e^-$ ELASTIC

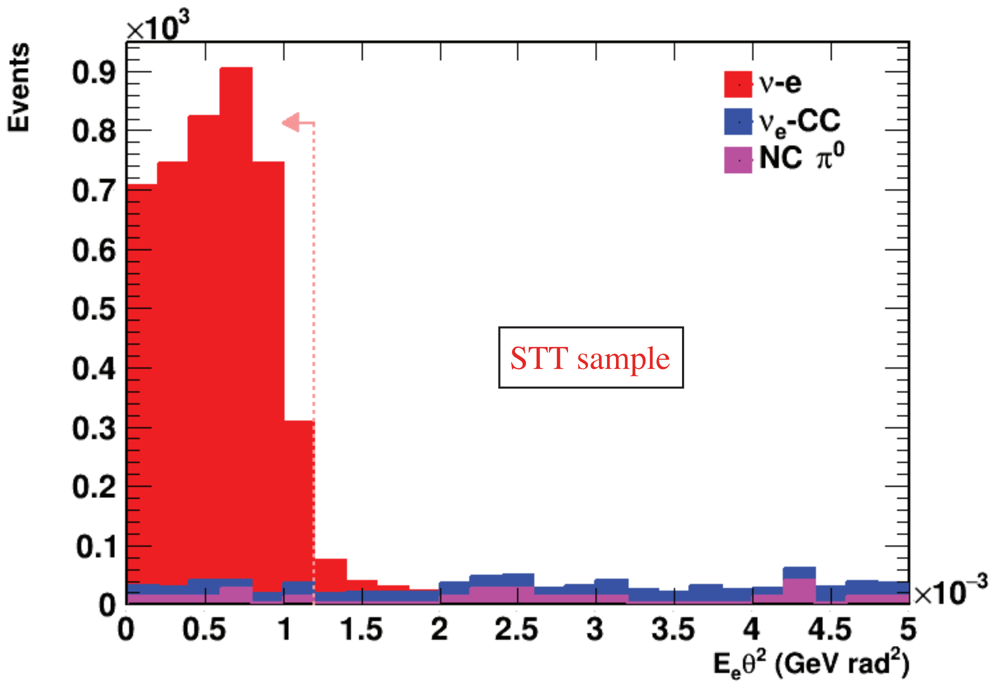


*1,162 (938) $\nu e^-$/year selected in FHC (RHC) beam from $CH_2$, C, Ar targets & straw mass*

✦ *Excellent electron ID, angular ($\sim 1.5$ mrad) and $E_e$ resolutions:*

| Detector | Signal | $\nu_e$ QE | NC $\pi^0$ | $\delta_{\rm stat}$ | $\delta_{\rm syst}$ | $\delta_{\rm tot}$ |
|---|---|---|---|---|---|---|
| SAND FHC 5y on-axis | 5,814 | 3% | 2% | 1.3% | ~1% | **~ 1.7%** |
| ND-LAr FHC + PRISM (50%) | 18,715 | 11% | 3% | 0.7% | ~1.5% | **~ 1.7%** |

$\Longrightarrow$ *Synergy of ND-LAr (syst. dominated) & SAND (stat. dominated) measurements*

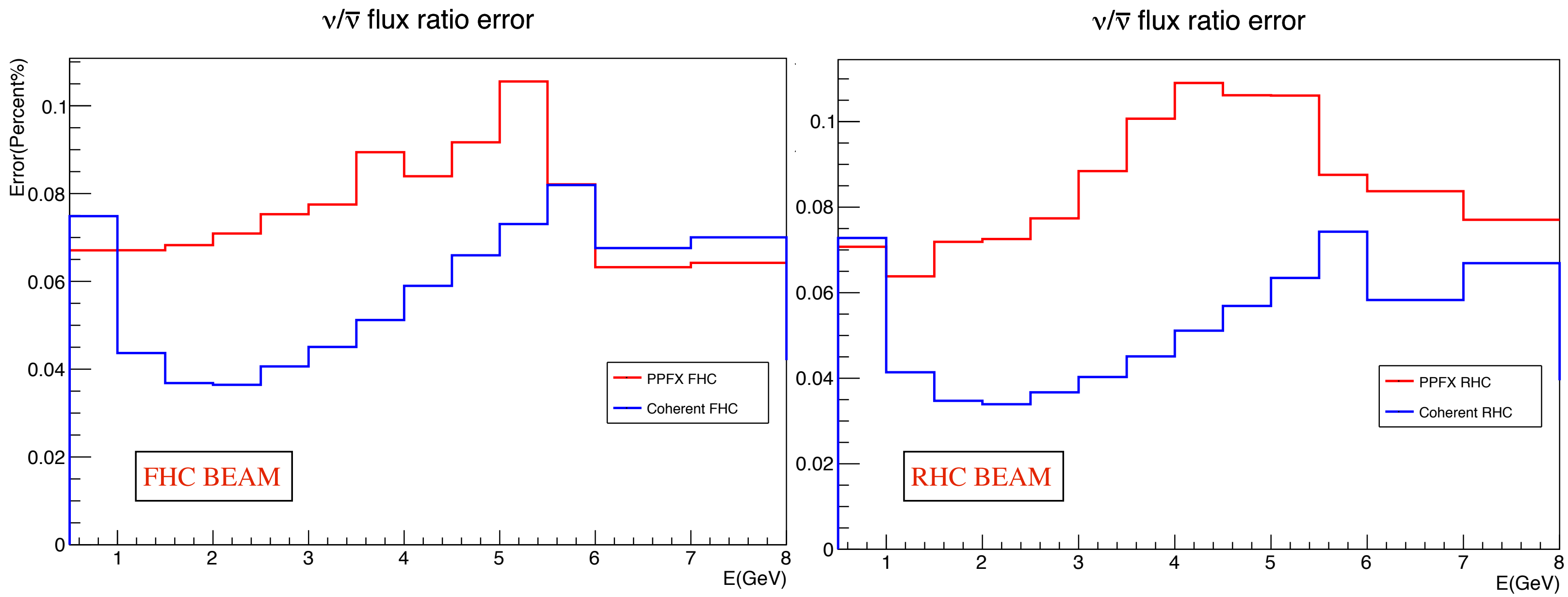


Figure 208: Uncertainty on the $\bar{\nu}_\mu/\nu_\mu$ flux ratio determined in STT from the ratio of coherent pion production in both the neutrino FHC (left panel) and antineutrino RHC (right panel) beam polarities. The corresponding uncertainties obtained from the beam simulation group are also shown for comparison.